Calcareous Smectite Clay as a Pozzolanic Alternative to Kaolin

Tobias Danner [a *], Geir Norden [b], Harald Justnes [a]

* Corresponding author: tobias.danner@sintef.no

[a] SINTEF Building materials and structures, Høgskoleringen 7B, 3, 7034 Trondheim, Norway

[b] Saint-Gobain Weber, 216 Alnabru, 0614 Oslo, Norway

Reference to the article can be made as followed:

T. Danner, G. Norden, H. Justnes; Calcareous Smectite Clay as a Pozzolanic Alternative to Kaolin; European Journal of Environmental and Civil Engineering, 2019, https://doi.org/10.1080/19648189.2019.1590741

Calcareous Smectite Clay as a Pozzolanic Alternative to Kaolin

The hydration of cement pastes with addition of a kaolinite rich clay (Clay A) and a calcareous smectite rich clay (Clay B) was investigated with isothermal calorimetry, in-situ XRD, PXRD, TGA and EPMA. Portland cement was replaced by 20, 35 and 50 weight% calcined clay in cement pastes and mortars. Both clays showed good pozzolanic reactivity. However, clay A having a higher amount of metakaolin and higher specific surface was more reactive in terms of CH consumption and mortar strength development. 50% replacement of PC by calcined Clay A resulted in increased 28 day compressive strength while mortars with 50% calcined Clay B showed almost equal 28 day compressive strength compared to the reference. With increasing addition of calcined clay, the second aluminate reaction (formation of AFm phase) of cement hydration was accelerated and the cement pastes became under sulphated. This resulted in a stronger and earlier sulphate depletion peak, especially in pastes with calcined Clay A. Due to 3% calcite in the used cement the main hydration product found was carboaluminate hydrate. The favoured formation of carboaluminate hydrate stabilised ettringite in the cement pastes.

Keywords: Pozzolana; cement; hydration; in-situ XRD, compressive strength

1 Introduction

Taking into account all steps from raw material mining to the final product, cement production is a highly energy intensive process, contributing 5-7% of the worldwide carbon dioxide emissions (Ernst Worrell, Lynn Price, Nathan Martin, Chris Hendriks, & Meida, 2001; Mehta, 1999). The most effective way of reducing CO_2 emissions in the short and long term is the replacement of parts of the clinker content with supplementary cementitious materials (SCMs) (Damtoft, Lukasik, Herfort, Sorrentino, & Gartner, 2008; Ernst Worrell, et al., 2001; Schneider, Romer, Tschudin, & Bolio, 2011). In the long term, large enough availability and sufficient reactivity, will determine the choice of suitable SCM sources (Gartner, 2004). The availability of the most common used SCM's, i.e. slag and fly ash, is limited compared to the production of cement and might decrease further in the future. Due to the widespread availability of calcined natural clays, this type of SCM has high potential to serve the cement industry sufficiently for a more sustainable future (K Scrivener, 2015).

In dependence of the clay mineralogy, calcination between 600-800°C, leads to the formation of amorphous or disordered metastable phases with high pozzolanic activity (Fernandez, Martirena, & Scrivener, 2011). Among the different clay minerals, kaolinite is proven to have the highest pozzolanic reactivity when calcined at the optimum temperature. Therefore, the pozzolanic reactivity of metakaolin was subject of detailed studies e.g. (Ambroise, Maximilien, & Pera, 1994; F. Avet and Scrivener, 2018b; De Silva and Glasser, 1992; El-Diadamony, Amer, Sokkary, & El-Hoseny, 2016; Frías and Cabrera, 2001; Jones, 2002; Mlinárik and Kopecskó, 2013; Sabir, Wild, & Bai, 2001; Siddique and Klaus, 2009; Tironi et al., 2014; Tironi, Scian, & Irassar, 2015; Tironi, Trezza, Scian, & Irassar, 2012). Kaolin clays with high purity are scarcely available and at the same time important raw materials for other industries. Consequently, there is a regaining interest in investigating poly-mineral clays containing different clay and non-clay minerals. With growing interest of using

calcined natural clays in the construction industry, the evaluation of the pozzolanic potential of local impure clays is getting more attention (Al-Rawas, Hago, Al-Lawati, & Al-Battashi, 2001; Almenares Reyes, Díaz, Rodríguez, Rodríguez, & Hernández, 2018; Alujas, Almenares, Betancourt, & Leyva, 2015; Aras, Albayrak, Arikan, & Sobolev, 2007; Berriel et al., 2016; Beuntner and Thienel, 2015; Chakchouk, Samet, & Mnif, 2006; Huenger, Gerasch, Sander, & Brigzinsky, 2018; Pöllmann, Da Costa, & Angelica, 2015; Shayma'a, Malath, Dalya Kh, Firas, & Abdul Wahab, 2012; Tironi, et al., 2012). It was shown that low grade kaolinitic clays with only 40% kaolinite content and high amounts of impurities of non-clay minerals like quartz and feldspars, can have sufficient pozzolanic reactivity (Alujas, et al., 2015; Aras, et al., 2007; François Avet, Snellings, Alujas Diaz, Ben Haha, & Scrivener, 2016; Tironi, et al., 2012). The pozzolanic reactivity of calcined natural clays was shown to increase with increasing amount of kaolinite (François Avet, et al., 2016; Chakchouk, et al., 2006). The coupled substitution of cement with calcined clay and limestone was also investigated (Antoni, Rossen, Martirena, & Scrivener, 2012; F. Avet and Scrivener, 2018a, 2018b; Bishnoi and Maity, 2018; Cancio Díaz et al., 2017; Favier, Zunino, Katrantzis, & Scrivener, 2018; Kunther, Dai, & Skibsted, 2015; Nied, Stabler, & Zajac, 2015; Karen Scrivener, Martirena, Bishnoi, & Maity, 2017; Tironi, et al., 2015). It was found that up to 45% substitution of cement with a 2:1 blend of metakaolin and limestone gave better compressive strength than the pure reference cement system (Antoni, et al., 2012). The good performance was explained by a strong synergistic effect between calcined clay and limestone (Antoni, et al., 2012; Nied, et al., 2015).

Only few studies covered investigations on natural clays already containing high amounts of calcium carbonate. Calcareous clay is not suitable for production of burnt clay products (e.g. bricks and light weight aggregate) due to the decomposition of $CaCO_3$ to CaO after burning. During service CaO may react with moisture to form $Ca(OH)_2$ which can result

in so called “pop outs“. Thus, these types of clays are not yet exploited by other industries and can serve as a large SCM resource to produce blended cements.

A recent study showed that marl (47% calcium carbonate in the raw material) can be a good pozzolanic material when calcined between 400-800 °C (Rakhimov, Rakhimova, Gaifullin, & Morozov, 2017). The present authors have previously published extensive studies on the pozzolanic activity of smectite rich clay containing 20-25% calcium carbonate, for simplicity called calcined "marl". (Danner, Justnes, Norden, & Østnor, 2015; Danner, Justnes, & Ostnor, 2012; Danner, Østnor, & Justnes, 2013; Justnes and Østnor, 2014; Østnor, Justnes, & Danner, 2015).

In this paper, the hydration of cement pastes with addition of two natural clays is investigated. Cement hydration of pastes with a kaolinite rich clay is compared to pastes with a calcareous smectite rich clay. Most smectite rich clays are known to have lower pozzolanic reactivity compared to kaolinite rich clays (Fernandez, et al., 2011). This paper shows that smectite rich clays containing calcium carbonate can be an effective pozzolanic material, comparable to natural kaolin, which enables pozzolanic cements with up to 55% clinker replacement (CEM IV/B) considering the 28 days compressive strength in mortars.

2 Materials and Experiments

2.1 Materials

Table 1 and Table 2 show the bulk mineralogy of crystalline phases of raw Clay A and Clay B determined with Rietveld analysis, and the chemical composition of the clays calcined at 800°C. The main mineral phases of Clay A are kaolinite, quartz and feldspar. Clay B is a smectite rich clay, with 25% calcite and 8% kaolinite. Norcem standard cement (CEM I 42.5 R) was used for mixing pastes of cement and calcined clay. The chemical composition is given in Table 2. The used cement contained 3% limestone. Pyrite was detected with XRD in Clay B, however, the chemical composition showed no SO_3. Under the SEM pyrite framboids were found in the raw clay indicating very localised distribution of pyrite (Danner, Norden, & Justnes, 2018). The sulphur from pyrite might have been removed during the calcination process. Heating of pyrite between 600-1000ºC with the addition of air results in decomposition of pyrite and the formation of iron oxides and sulphur dioxide gas (Runkel and Sturm, 2009). A detailed characterisation of both clays in the raw and calcined state, including the XRD spectra of the starting clay, can be found in (Danner, et al., 2018).

Table 1 and Table 2

2.2 Production of calcined Clays

The calcination of Clay A and B was performed in a direct natural gas heated rotary kiln at IBU-tec advanced materials AG (Weimar, Germany). The kiln is designed for a continuous thermal treatment and was used to simulate trials under industrial conditions. The feed rate was 30 kg/h and the residence time in the kiln was 45 min. The clays were calcined at different temperatures between 600-1100°C and their pozzolanic reactivity was investigated in dependence of the temperature (Danner, et al., 2018). Clay B showed highest pozzolanic

reactivity at 800°C. Clay A already showed high pozzolanic reactivity when burned at 700°C. However, the pozzolanic reactivity was relatively constant between 700 to 800°C (Danner, et al., 2018). Therefore, this paper, compares results for both clays burned at 800°C. Changes in microstructure and phase assemblage upon calcination of the clays are reported in detail in (Danner, et al., 2018).

The calcined clay lumps were milled down with a discontinuous drum mill to a d_{50} < 10 µm at UVR-FIA GmbH (Freiberg, Germany).

2.3 Quantitative mineralogical analysis of the raw clays using X-Ray Diffraction (XRD)

Bulk mineralogy of natural Clay A and B was performed with XRD on dried and ground samples using the back-loading sample preparation technique. The ≤ 2 µm fraction (clay fraction) was separated from the bulk sample by means of sedimentation, smeared on a glass plate and dried in air. The clay fraction was investigated under three different conditions (a-c); a: untreated, b: after treatment with ethylene glycol vapours in a desiccator for 24 h at 60°C, c: after heating at 500°C for 1 h. For analysis, a PAN Analytical X'Pert Pro MPD equipped with a X'Celerator RTMS detector, an automatic divergence slit and a Cu-Kα X-ray source was used. The samples were measured from 2-65° 2θ using a step size of 0.0170° 2θ and a step time of 20 sec. Data was collected at 45 kV and 40 mA. More details on the procedure of quantitative mineralogical analysis can be found in (Nielsen, 1994; Nielsen, Cremer, Stein, Thiébault, & Zimmermann, 1989).

2.4 X-Ray Fluorescence (XRF)

XRF analysis was performed with a Bruker AXS S8 Tiger WDXRF equipped with a 4 kW generator. Dried and powdered clay samples were ignited at 850°C. Dried clay sample (0,5 g)

was added to a 2:1 mix of lithium- tetraborate and metaborate (5 g) and lithium iodide (60 µg). The mixture was fused in a platinum crucible and moulded to a glass disk.

2.5 Mixing of Pastes

Portland cement (PC) was dry mixed with 20, 35 and 50 weight% calcined clay and homogenized by hand. Deionized water was added, and the paste was mixed for 1 minute by hand with a plastic spatula. The water to binder ratio was 0.5 and the pastes were hydrated for 28 days at 20°C. The hydration was stopped by washing the pastes with ethanol, crushing by hand and drying the samples in a desiccator above saturated $CaCl_2$-solution (RH about 33%).

2.6 Isothermal Calorimetry

Isothermal calorimetry of cement pastes was carried out at 20°C using a TAM Air (TA Instruments). About 6 g of paste were weighed accurately and used for each measurement. Mixing was performed outside the calorimeter by hand with a plastic spatula for 1 min. The cumulative heat of cement pastes was determined with an accuracy of ± 0.5 J/g.

2.7 In situ XRD

In-situ XRD was performed using a Bruker D8 Advance, equipped with Cu-Kα radiation and a Vantec-1 position sensitive detector. The cement pastes were smeared in the sample holder and the sample surface was flattened by stripping off the excess material with a glass plate. About 1 g of paste was used for each measurement. The sample was then placed in an MRI Physikalische Geräte GmbH sample chamber, and data was collected at room temperature (20°C) and constant relative humidity of 96%. The measurements started about 3 ± 1 min after mixing. One scan took about 13 min, and a total of 110 scans were collected during 24 h.

Results are shown in form of 2-D level plots where intensities of appearing phases are visualized by a colour gradient (Danner, Justnes, Geiker, & Lauten, 2015).

2.8 Powder X-Ray diffraction (PXRD)

Dried samples of hydrated cement paste were finely ground with a hand mortar and prepared for XRD measurements using the front loading technique. The samples were measured with a D8 Focus diffractometer from Bruker equipped with a Lynx Eye detector and a Cu-Kα X-Ray source. A fixed divergence slit of 0.2 mm was used. Measurements were taken from 5-65° 2θ with a step size of 0.2° 2θ and a step time of 1 sec.

2.9 Thermogravimetry (TG/DTG)

Thermogravimetric analysis was performed with a Mettler Toledo TGA/SDTA 851. Dried powdered samples of cement paste were analysed with a heating rate of 10°C/min between 40 – 1100°C in nitrogen atmosphere (30 ml/min flow rate). Prior to analysis, all samples were dried additionally for 2 h at 40°C inside the TGA apparatus to remove adsorbed water. The $Ca(OH)_2$ consumption after 28 days of hydration was calculated from the weight loss in the temperature interval of $Ca(OH)_2$ decomposition. The exact boundaries for the temperature interval of $Ca(OH)_2$ are read from the 1_{st} derivative curve (DTG). The weight loss calculated from the difference of the horizontal tangents in the TGA signal is multiplied with the molar ratio 74/18 to obtain $Ca(OH)_2$ from H_2O mass loss at about 500°C.

2.10 Electron Probe Micro Analysis (EPMA)

For EPMA analysis, hydrated paste samples were cast in epoxy resin, plane polished in iso-propanol and coated with carbon. The instrument used was a JEOL JXA-8500F Electron Probe Micro Analyser (EPMA). The JEOL JXA-8500F instrument is equipped with 5 wavelength

dispersive X-ray spectrometers (WDS) and an energy dispersive X-ray spectrometer (EDS). All samples were investigated in the backscattered electron imaging (BEI) modus with an accelerating voltage of 15 kV.

2.11 Compressive Strength

Mortars were prepared by substituting Portland cement (PC) with 20, 35 and 50 weight% calcined clay. The mixing procedure was according to the Norwegian Standard NS-EN 196-1 ("Standard CEN - EN 196-1 Methods of testing cement Part1: Determination of strength," 2005). The water to binder ratio (w/b) was held constant at 0.5 in all mortar mixes by using superplasticizer. The amount of superplasticizer used increased with increasing amount of cement replacement by calcined clay. In mixes containing 50% calcined Clay A and B, 1.5 and 1% superplasticizer by weight of binder was added. The consistency of fresh mortar was determined using a flow table and the flow of mortars containing calcined clay was within ± 5% of the reference mortar. The mortar mixes were cast in three 40x40x160 mm moulds and stored in a cabinet for 24 hours at 23 ± 2°C and 90% relative humidity (RH). After 24 hours, the mortar prisms were removed from the moulds and stored in saturated CH water to avoid leaching. The compressive strength was determined after 1, 3, 7 and 28 days according to the Norwegian Standard NS-EN 196-1.

3 Results and Discussion

3.1 Isothermal Calorimetry

The curves of thermal power and cumulative heat development up to 35 hours of hydration of the cement pastes blended with Clay A and Clay B are shown in Figure 1 and Figure 2, respectively.

The thermal power curve (i.e. heat of hydration rate evolution) of PC without calcined clay showed the typical behaviour for cement hydration. After the induction period, which ended between 3-4 hours, two exothermic peaks related to the acceleration period appeared. The first maximum after 9-10 hours is associated to the silicate reaction, i.e. the formation of C-S-H and CH from hydration of C_3S and C_2S. The second maximum in the acceleration period appeared after about 15 hours and is associated to the aluminate reaction, i.e. a combination of renewed ettringite formation and the conversion of Aft (ettringite) to AFm (mono-sulphate) phases (Taylor, 1997). The second maximum in the acceleration period is also referred to as the sulphate depletion peak (Jansen, Goetz-Neunhoeffer, Lothenbach, & Neubauer, 2012). When PC was blended with Clay A or B the two maxima in the acceleration period appeared stronger and earlier with increased substitution of cement by calcined clay. The time between the two maxima in the acceleration period seemed also to decrease with increasing replacement level of PC. The effect was more pronounced for cement pastes mixed with Clay A. The times of appearance of the second maxima (t_{max}= time of maximum thermal power) in the acceleration period are given in Table 3 for the different cement pastes.

A similar change in kinetics was observed in literature for cements blended with metakaolin, silica fume or calcined marl (Antoni, et al., 2012; Fernandez Lopez, 2009; Ng and Justnes, 2015a, 2015b; Rahhal and Talero, 2008; Rossen, Lothenbach, & Scrivener, 2015; Talero and Rahhal, 2009). The substitution of cement by calcined clay mainly affects the aluminate reaction. The high specific surface area of calcined clays significantly modifies the

reactivity of the aluminate phases. Additionally, with increasing levels of calcined clay, the systems get under sulphated which also causes the sulphate depletion peak to shift to earlier times. The higher the content of metakaolin the earlier and more distinct is the sulphate depletion peak (Antoni et al., 2012). Clay A contains 47% metakaolin compared to 8% in Clay B explaining the increased acceleration of nucleation in pastes with Clay A (Antoni et al., 2012). Besides 8% metakaolin, Clay B also contains about 50% meta-smectite which contributes to reactivity, however, less than metakaolin. Metakaolin contains more reactive alumina compared to meta-smectite which is why cement pastes with Clay A appear considerably more under-sulphated than pastes with Clay B. Antoni et al., 2012 observed that at very high levels of PC replacement, the sulphate depletion peak might occur before the main silicate reaction. Sulphate optimisation by adding additional sulphates to the system could move the sulphate depletion peak back to later times (Antoni et al., 2012). It was also shown that the higher heat flow and enhanced aluminate reaction can be related to the so called filler effect (Lothenbach, Scrivener, & Hooton, 2011). The calcined clays act as nucleation sites and promote the nucleation of the hydrates forming. Besides the higher kaolinite content and thus the higher amount of reactive alumina, Clay A contains a higher amount of inert phases (e.g. quartz and feldspar) compared to Clay B (Table 1 and Table 2). Clay B calcined at 800ºC contains only about 5% calcite compared to 25% in the raw clay before calcination (Danner et al., 2018). The inert phases of clay A do not change upon calcination. Consequently, calcined Clay A contains about 50% filler minerals compared to about 10% in calcined Clay B.

3.2 In-situ XRD

Feil! Fant ikke referansekilden. shows the in-situ XRD level plot of the pure PC paste hydrated for 24 h. Partly dissolution of the clinker grains C_3S/C_2S and C_3A is visible in the decreasing intensities between 29-42°2θ. Continuous ettringite (AFt) formation can be

observed at 9.1, 15.7 and 22.9° 2θ from the first minutes. After about 11 h, the formation of crystalline portlandite (CH) was detected. The time of portlandite detection correlated with the time of the start of the sulphate depletion peak in isothermal calorimetry (Figure 1 and Figure 2).

Figure 4 shows the in-situ XRD level plot of hydration of cement paste blended with 20% Clay A, together with the thermal power curve. At 10.8° 2θ the formation of an AFm phase was detectable after about 12.5 h. The peak positions (10.8 and 21.7° 2θ) indicate the presence of hemi-carboaluminate hydrate. In the pure PC paste the formation of hemi-carboaluminate hydrate was not detected during the first 24 hours of hydration. The time of hemi-carboaluminate detection was associated with the peak of the sulphate depletion in the acceleration period of the thermal power curve. In the cement pastes blended with calcined clay the aluminate reaction, here the formation of hemi-carboaluminate hydrate appeared to be accelerated. Ettringite did not disappear with the formation of hemi-carboaluminate hydrate. Ettringite stabilization by favoured formation of carboaluminate hydrate AFm phases in systems containing limestone is a well-known effect (De Weerdt, Kjellsen, Sellevold, & Justnes, 2011). As mentioned earlier, the cement used in this study contained about 3% limestone which enabled the formation of carboaluminate hydrate phases even in the system with Clay A. In the cement paste containing 20% calcined Clay A the precipitation of CH was accelerated by about 2 h compared to the pure PC paste. The time of first detection of CH was again associated with the start of the sulphate depletion peak in the thermal power curve. The results show that the silicate and aluminate reaction of cement hydration were accelerated.

Sections of the in-situ XRD level plots of cement pastes blended with 20, 35 and 50% Clay A hydrated for 24 h, are given in Figure 5. The formation of hemi-carboaluminate hydrate was accelerated with increased amount of calcined clay in the cement paste. The time of first detection of hemi-carboaluminate was after about 9 and 7 h in cement pastes with 35 and 50 %

Clay A, respectively. This was again in good agreement with the peak time of the sulphate depletion peak in the thermal power as given in Table 3.

Cement pastes blended with Clay B showed a similar behaviour as cement pastes blended with Clay A, however, not to the same extent. As mentioned above this can be explained by the lower amount of metakaolin, and hence the lower amount of reactive alumina. The main precipitation of hemi-carboaluminate was associated to the sulphate depletion peak in the acceleration period. Additionally, in all cement pastes with calcined Clay B, the formation of CH correlated with the start of the sulphate depletion peak. Again, both the aluminate and silicate reaction appeared to be accelerated with increasing amount of calcined clay in the paste.

3.3 Powder X-ray diffraction of hydrated Cement Pastes (PXRD)

Figure 6 shows the diffractograms of cement pastes with 0, 20, 35 and 50% replacement of cement by calcined Clay A (left) and calcined Clay B (right) hydrated for 28 days at 20°C. The hydration products formed in cement pastes blended with calcined Clay A were ettringite, carboaluminate hydrates and strätlingite. Strätlingite was first formed in the paste containing 35% calcined clay. At least 30% of PC have to be replaced by metakaolin to form crystalline strätlingite (Ambroise, et al., 1994) because strätlingite is not stable in presence of calcium hydroxide (Okoronkwo and Glasser, 2016). Carboaluminate hydrates formed due to a reaction of AFm phases with the limestone contained in the cement. Besides the decreasing level of limestone in the pastes with higher addition of calcined Clay A, the amount of hemi-carboaluminate hydrate increased with increasing level of cement replacement. Increased addition of calcined Clay A results in an increased amount of metakaolin and thus an increased amount of reactive alumina to form AFm phases. The in total higher amount of AFm phases in the system can react with the limestone, consequently forming a higher amount of hemi-

carboaluminate hydrate. Thus, the formation of carboaluminate hydrate is limited by the amount of reactive alumina more than the availability of limestone. Still, due to the limiting amount of limestone at high replacement levels a favoured formation of hemi-carboaluminate occurred. With 50% calcined clay, almost all calcium hydroxide was consumed after 28 days. Moreover, with increasing clay content a new peak at 8.9 °2θ, to the left side of ettringite, appeared. This peak could possibly be assigned to muscovite present in Clay A. The mineral structure of muscovite is not much affected by the heat treatment at 800°C and becomes more and more visible with increasing clay content in the pastes. However, the peak intensities do not increase proportionate from 20 to 35% cement replacement. At present, it is not clear to which phase the peak belongs to.

The crystalline hydration products observed in cement pastes blended with calcined Clay B after hydration for 28 days at 20ºC were similar to the phases detected in pastes with Clay A, with the exception that strätlingite did not form. With 20% addition of calcined Clay B the amount of carboaluminate hydrates increased. Further increase of calcined Clay B appeared to result only in a minor increase of the amount of carboaluminate hydrates. Compared to Clay A, Clay B contains less reactive alumina and thus forms in total less AFm phases. In pastes with calcined Clay B, higher amounts of mono-carboaluminate formed relative to hemi-carboaluminate as observed in pastes with calcined Clay A. The favoured formation of mono-carboaluminate in pastes with Clay B can be explained by the additional content of limestone in Clay B. Due to the pozzolanic reaction, the CH content decreased as the amount of carboaluminate hydrates increased, but CH was not depleted even with an addition of 50% Clay B. Ettringite was still stable after 28 days of hydration and no conversion to monosulphate phases was found. As mentioned earlier the favoured formation of carboaluminate hydrates in systems with limestone results in a stabilization of ettringite (De Weerdt, et al., 2011; Lothenbach, Le Saout, Gallucci, & Scrivener, 2008).

3.4 Thermogravimetry (TG/DTG)

The DTG curves of cement pastes blended with Clay A and Clay B after hydration for 28 days at 20°C are shown in Figure 7. Both systems showed four major peaks at around 130, 190, 490 & 700-800°C. These peaks are associated with the decomposition of ettringite and C-S-H (130°C), carboaluminate hydrate (190°C), calcium hydroxide (490°C) and calcite (700-800°C). In addition, both systems showed a small shoulder around 250°C and a small peak around 370°C. These signals are typically observed in hydrating cementitious systems and are commonly associated with the decomposition of AFm phases like carboaluminate hydrates (Lothenbach, Durdzinski, & De Weerdt, 2015; Ramachandran, 1988). It can be seen, that the amount of formed carboaluminate increased with increasing clay content in the cement pastes while the amount of ettringite appeared rather stable. The CH content was significantly reduced after 28 days of hydration in the cement pastes containing calcined clays. Pastes containing calcined Clay A produced a higher amount of carboaluminate hydrate compared to pastes with Clay B. It can also be seen that calcined Clay A consumed more CH than calcined Clay B due to the higher amount of reactive material (metakaolin). The amount of CH after 28 days of hydration at 20°C was calculated from the TG curves and is given in Table 4. Pure PC produced about 16% CH after hydration for 28 days at 20°C. With increased amount of calcined clay the amount of CH after 28 days was reduced. It is shown that Clay A consumed more CH in the cement paste compared to Clay B at similar levels of addition. With 50% calcined Clay A only about 2% CH were left in the paste after 28 days of hydration at 20°C, assuming that no other hydrates decompose in the CH range. As comparison about 5% CH was left in pastes with 50% calcined Clay B. The results show that both clays are very effective pozzolanic materials

3.5 Electron Probe Micro Analysis (EPMA)

Figure 8 and Figure 9 show backscattered electron (BSE) images of the cement pastes blended with 20, 35 and 50% calcined Clay A and Clay B, respectively, after hydration for 28 days at 20°C. Point analysis was performed in different locations marked with numbers 1-8. The WDX compositions measured in these points is given in atomic% in Table 5. The microstructure of all pastes appeared very dense. Larger grains of quartz and feldspars from the clays and grains of more or less hydrated clinker phases were found in a matrix of finer crystalline hydration products. With increasing amount of calcined clay in the pastes, the amount of CH observed was decreasing. In pastes with Clay A, strätlingite was the main hydration product to be detected. At higher replacement levels (Figure 8c) cross sections of strätlingite platelets were found all over the matrix. In the cement paste blended with 20% Clay A strätlingite could be found in voids but seemed to be less crystalline (Figure 8a). The average composition of Points 1, 3, 4 & 5 was Ca = 11.9, Al = 9.9 and Si = 5.9. The ratio of Ca/Al=1.2 and Ca/Si=2.0 correlates well with the composition of strätlingite.

The long needles visible in pastes with calcined Clay B (Figure 9a) might represent ettringite from the cement hydration. The needles were too thin to be analysed with WDX. In voids of the matrix, crystalline Ca-Al hydrates were detected (Figure 9a-c). The measured composition of points 6-8 is given in Table 5 The Ca/Al ratio varies from 1.9 in point 6 to 2.8 in point 8. Point 6 and 7 most likely represent carboaluminate AFm phases with iron and silicon substitution in the structure, while point 8 might be assigned to Fe-substituted ettringite (Danner, 2013).

3.6 Compressive Strength

Figure 10 shows the compressive strength development of standard mortars from 1 to 28 days, with 20, 35 and 50% replacement of PC by calcined Clay A. The error of compressive strength results from mortar tests was about ± 1MPa. At 1 day curing the compressive strength of the

400 mortars was reduced with increasing replacement level of PC. Still, already after 3 days the
401 mortar with 20% replacement of PC by calcined Clay A achieved a similar compressive
402 strength than the reference. After 7 days, mortars with 20 and 35% calcined Clay A showed
403 26% and 9% higher compressive strength than the reference. After 28 days curing, even the
404 mortar mix containing 50% calcined Clay A had a higher strength than the reference. The 28
405 day compressive strength was increased by 23, 15 and 9% respectively, when PC was replaced
406 with 20, 35 and 50 calcined Clay A (Table 6).

407 Figure 11 shows the compressive strength development of standard mortars from 1 to
408 28 days, with 20, 35 and 50% replacement of PC by calcined Clay B. It should be noted that
409 the strength of the reference mortar with 100% PC was higher than for the tests made with Clay
410 A. The reason for this is that the tests were performed at different times, and thus, different
411 batches of the same cement were used. Consequently, when comparing the strength
412 development of mortars with Clay A to mortars with Clay B, the relative strength development
413 should be compared. After curing for 1 and 3 days, the compressive strength of the mortars
414 was reduced the higher the replacement level of PC by calcined clay. Nevertheless, the 1 day
415 strength of the mortar with 50% replacement by Clay B was about 10 MPa, which is sufficient
416 for removing formwork of concrete in practice. After 7 days curing, the compressive strength
417 of mortars with 20 and 35% replacement was 95 and 92% of the reference strength. At 28 days,
418 the mortars with 20 and 35% addition of calcined Clay B had a 7 and 6% higher compressive
419 strength than the reference. With 50% replacement of PC by calcined Clay B the strength was
420 with 95% almost equal to the reference.

421 Table 6 and Table 7 show the relative strength of mortars with 20, 35 and 50%
422 replacement of PC by calcined Clay A and calcined Clay B after 1, 3, 7 and 28 days of curing.
423 As described before, the systems are under-sulphated at high replacement levels which might
424 reduce the early age strength of the mortars. Sulphate optimisation could increase the early age

strength. In a different study, it was shown that 1 day compressive strength of systems with 45% cement replacement by a metakaolin and limestone blend can be increased by adding extra calcium sulphate (Antoni, et al., 2012). Comparing the relative strength of the mortars after 1day curing, there seems to be no significant difference between the strength development of mortars with Clay A and mortars with Clay B. From 3-28 days the mortars containing 20 and 35% calcined Clay A had a considerable higher relative compressive strength than the mortars containing 20 and 35% calcined Clay B. This can be explained by the higher reactivity of calcined Clay A containing a higher amount of metakaolin. Calcined Clay B has a total higher amount of clay minerals with 53% smectite and 8% kaolin. Due to this, calcined Clay B showed also pozzolanic reactivity. However, the meta-smectite in calcined Clay B is less reactive than metakaolin which seems to slow down the reactions compared to Clay A. At high replacement levels of 50% the early compressive strength (1-7 days) is reduced. With decreased level of cement the amount of CH produced and being available for reaction with the calcined clays is reduced. Furthermore, besides increasing the amount of reactive clay minerals, the amount of inert phases is increased with increased addition of calcined clay.

4 Conclusions

The hydration of cement pastes with addition of a kaolinite rich clay (Clay A) and a calcareous smectite rich clay (Clay B) was investigated with isothermal calorimetry, in-situ XRD, PXRD, TGA and EPMA. Portland cement was replaced by 20, 35 and 50 weight% calcined clay in cement pastes and mortar tests.

The following conclusions can be drawn.

- Due to the higher amount of metakaolin and the higher specific surface, calcined Clay A showed highest pozzolanic reactivity in terms of CH consumption and mortar strength development. Mortars with 20, 35 and 50% PC replacement by calcined Clay A showed higher 28 day compressive strength compared to the reference.
- The calcareous smectite rich Clay B demonstrated good pozzolanic activity but appeared to react slower than Clay A. Considering the 28 days strength and sufficient early strength of mortars, calcareous smectite clays may enable pozzolanic cements with up to 55% clinker replacement (CEM IV/B).
- With increasing addition of calcined clay the second aluminate reaction (formation of AFm phase) of cement hydration was accelerated and the cement pastes became under sulphated. This resulted in a stronger and earlier sulphate depletion peak, especially for pastes with calcined Clay A.
- Due to 3% calcite in the used cement the main hydration product found in pastes with calcined Clay A was hemi-carboaluminate hydrate. Due to additional calcite in calcined Clay B, the formation of mono-carboaluminate hydrate was favoured in pastes with high additions of calcined Clay B. The favoured formation of carboaluminate hydrate stabilised ettringite in the cement pastes.

Acknowledgement

Saint-Gobain Weber is acknowledged for initiating and financing this research project. SINTEF Building and Infrastructure is acknowledged for the cooperation, support with mortar testing and discussing the results of this research. Julian Tolchard from SINTEF Industry is acknowledged for help with setting up the XRD instrument for in-situ measurements. Prof. Ole Bjørnslev Nielsen (University of Aarhus, Denmark) is acknowledged for performing the mineralogical analysis of the raw clays.

References

Al-Rawas, A. A., Hago, A. W., Al-Lawati, D., & Al-Battashi, A. (2001). The Omani artificial pozzolans (sarooj). *Cement, concrete and aggregates, 23*(1), pp. 19-26.

Almenares Reyes, R. S., Díaz, A. A., Rodríguez, S. B., Rodríguez, C. A. L., & Hernández, J. F. M. (2018). *Assessment of Cuban Kaolinitic Clays as Source of Supplementary Cementitious Materials to Production of Cement Based on Clinker – Calcined Clay – Limestone.* Dordrecht.

Alujas, A., Almenares, R. S., Betancourt, S., & Leyva, C. (2015). Pozzolanic reactivity of low grade kaolinitic clays: influence of mineralogical composition *Calcined Clays for Sustainable Concrete* (pp. 339-345): Springer.

Ambroise, J., Maximilien, S., & Pera, J. (1994). Properties of metakaolin blended cements. *Advanced Cement Based Materials, 1*(4), pp. 161-168.

Antoni, M., Rossen, J., Martirena, F., & Scrivener, K. (2012). Cement substitution by a combination of metakaolin and limestone. *Cement and Concrete Research, 42*(12), pp. 1579-1589.

Aras, A., Albayrak, M., Arikan, M., & Sobolev, K. (2007). Evaluation of selected kaolins as raw materials for the Turkish cement and concrete industry. *Clay Minerals, 42*(2), pp. 233-244. doi:10.1180/claymin.2007.042.2.08 Retrieved from http://www.ingentaconnect.com/content/minsoc/cm/2007/00000042/00000002/art00008 https://doi.org/10.1180/claymin.2007.042.2.08

Avet, F., & Scrivener, K. (2018a). *Hydration Study of Limestone Calcined Clay Cement (LC3) Using Various Grades of Calcined Kaolinitic Clays.* Dordrecht.

Avet, F., & Scrivener, K. (2018b). *Reaction Degree of Metakaolin in Limestone Calcined Clay Cement (LC3).* Dordrecht.

Avet, F., Snellings, R., Alujas Diaz, A., Ben Haha, M., & Scrivener, K. (2016). Development of a new rapid, relevant and reliable (R3) test method to evaluate the pozzolanic reactivity of calcined kaolinitic clays. *Cement and Concrete Research, 85*, pp. 1-11. doi:https://doi.org/10.1016/j.cemconres.2016.02.015 Retrieved from http://www.sciencedirect.com/science/article/pii/S0008884616302368

Berriel, S. S., Favier, A., Domínguez, E. R., Machado, I. S., Heierli, U., Scrivener, K., . . . Habert, G. (2016). Assessing the environmental and economic potential of Limestone Calcined Clay Cement in Cuba. *Journal of Cleaner Production, 124*, pp. 361-369.

Beuntner, N., & Thienel, K. C. (2015). *Properties of Calcined Lias Delta Clay—Technological Effects, Physical Characteristics and Reactivity in Cement.* Dordrecht.

Bishnoi, S., & Maity, S. (2018). *Limestone Calcined Clay Cement: The Experience in India This Far.* Dordrecht.

Cancio Díaz, Y., Sánchez Berriel, S., Heierli, U., Favier, A. R., Sánchez Machado, I. R., Scrivener, K. L., . . . Habert, G. (2017). Limestone calcined clay cement as a low-carbon solution to meet expanding cement demand in emerging economies. *Development Engineering, 2*, pp. 82-91. doi:https://doi.org/10.1016/j.deveng.2017.06.001 Retrieved from http://www.sciencedirect.com/science/article/pii/S2352728516300240

Chakchouk, A., Samet, B., & Mnif, T. (2006). Study on the potential use of Tunisian clays as pozzolanic material. *Applied Clay Science, 33*(2), pp. 79-88.

Damtoft, J. S., Lukasik, J., Herfort, D., Sorrentino, D., & Gartner, E. M. (2008). Sustainable development and climate change initiatives. *Cement and Concrete Research, 38*(2), pp. 115-127. doi:https://doi.org/10.1016/j.cemconres.2007.09.008 Retrieved from http://www.sciencedirect.com/science/article/pii/S0008884607002153

Danner, T. (2013). *Reactivity of calcined clays, Doctoral Thesis, 2013:218* (Doctoral Thesis. Norwegian University of Science and Technology - NTNU.

Danner, T., Justnes, H., Geiker, M., & Lauten, R. A. (2015). Phase changes during the early hydration of Portland cement with Ca-lignosulfonates. *Cement and Concrete Research, 69*, pp. 50-60. doi:https://doi.org/10.1016/j.cemconres.2014.12.004 Retrieved from http://www.sciencedirect.com/science/article/pii/S0008884614002464

Danner, T., Justnes, H., Norden, G., & Østnor, T. (2015). Feasibility of Calcined Marl as an Alternative Pozzolanic Material *Calcined Clays for Sustainable Concrete* (pp. 67-73): Springer.

Danner, T., Justnes, H., & Ostnor, T. (2012). Calcined marl as a pozzolan for sustainable development of the cement and concrete industry. *ACI Special Publication, 289*

Danner, T., Norden, G., & Justnes, H. (2018). Characterisation of calcined raw clays suitable as supplementary cementitious materials. *Applied clay science, 162*, pp. 391-402.

Danner, T., Østnor, T. A., & Justnes, H. (2013). *Thermally activated marl as a pozzolan for cementitious based products.* Twin Covilha International Conference on Civil Engineering - Towards a better environment and The Concrete Future, Covilha, Portugal.

De Silva, P., & Glasser, F. (1992). Pozzolanic activation of metakaolin. *Advances in Cement Research, 4*(16), pp. 167-178.

De Weerdt, K., Kjellsen, K., Sellevold, E., & Justnes, H. (2011). Synergy between fly ash and limestone powder in ternary cements. *Cement and Concrete Composites, 33*(1), pp. 30-38.

El-Diadamony, H., Amer, A. A., Sokkary, T. M., & El-Hoseny, S. (2016). Hydration and characteristics of metakaolin pozzolanic cement pastes. *HBRC Journal*doi:https://doi.org/10.1016/j.hbrcj.2015.05.005 Retrieved from http://www.sciencedirect.com/science/article/pii/S1687404815000486

Ernst Worrell, Lynn Price, Nathan Martin, Chris Hendriks, & Meida, L. O. (2001). CARBON DIOXIDE EMISSIONS FROM THE GLOBAL CEMENT INDUSTRY. *Annual Review of Energy and the Environment, 26*(1), pp. 303-329. doi:10.1146/annurev.energy.26.1.303 Retrieved from http://www.annualreviews.org/doi/abs/10.1146/annurev.energy.26.1.303

554 Favier, A., Zunino, F., Katrantzis, I., & Scrivener, K. (2018). *The Effect of Limestone on the*
555 *Performance of Ternary Blended Cement LC3: Limestone, Calcined Clays and Cement.*
556 Dordrecht.
557 Fernandez Lopez, R. (2009). Calcined clayey soils as a potential replacement for cement in
558 developing countries.
559 Fernandez, R., Martirena, F., & Scrivener, K. L. (2011). The origin of the pozzolanic activity
560 of calcined clay minerals: A comparison between kaolinite, illite and montmorillonite.
561 *Cement and Concrete Research, 41*(1), pp. 113-122.
562 doi:https://doi.org/10.1016/j.cemconres.2010.09.013 Retrieved from
563 http://www.sciencedirect.com/science/article/pii/S0008884610002176
564 Frías, M., & Cabrera, J. (2001). Influence of MK on the reaction kinetics in MK/lime and MK-
565 blended cement systems at 20 C. *Cement and Concrete Research, 31*(4), pp. 519-527.
566 Gartner, E. (2004). Industrially interesting approaches to "low-CO2" cements. *Cement and*
567 *Concrete Research, 34*(9), pp. 1489-1498.
568 doi:https://doi.org/10.1016/j.cemconres.2004.01.021 Retrieved from
569 http://www.sciencedirect.com/science/article/pii/S0008884604000468
570 Huenger, K.-J., Gerasch, R., Sander, I., & Brigzinsky, M. (2018). *On the Reactivity of Calcined*
571 *Clays from Lower Lusatia for the Production of Durable Concrete Structures.*
572 Dordrecht.
573 Jansen, D., Goetz-Neunhoeffer, F., Lothenbach, B., & Neubauer, J. (2012). The early hydration
574 of Ordinary Portland Cement (OPC): An approach comparing measured heat flow with
575 calculated heat flow from QXRD. *Cement and Concrete Research, 42*(1), pp. 134-138.
576 doi:https://doi.org/10.1016/j.cemconres.2011.09.001 Retrieved from
577 http://www.sciencedirect.com/science/article/pii/S0008884611002328
578 Jones, T. R. (2002). Metakaolin as a pozzolanic addition to concrete. *Structure and*
579 *Performance of Cements*, pp. 372-398.
580 Justnes, H., & Østnor, T. (2014). *Durability and microstructure of mortar with calcined marl*
581 *as supplementary cementing material.* Proceedings of the XIII conference on Durability
582 of Building Materials and Components (DBMC), Sao Paulo, Brazil.
583 Kunther, W., Dai, Z., & Skibsted, J. (2015). *Thermodynamic Modeling of Portland Cement—*
584 *Metakaolin—Limestone Blends.* Dordrecht.
585 Lothenbach, B., Durdzinski, P., & De Weerdt, K. (2015). Thermogravimetric analysis. *A*
586 *Practical Guide to Microstructural Analysis of Cementitious Materials; Scrivener, K.,*
587 *Snellings, R., Lothenbach, B., Eds*, pp. 178-208.
588 Lothenbach, B., Le Saout, G., Gallucci, E., & Scrivener, K. (2008). Influence of limestone on
589 the hydration of Portland cements. *Cement and Concrete Research, 38*(6), pp. 848-860.
590 Lothenbach, B., Scrivener, K., & Hooton, R. D. (2011). Supplementary cementitious materials.
591 *Cement and Concrete Research, 41*(12), pp. 1244-1256.
592 doi:https://doi.org/10.1016/j.cemconres.2010.12.001 Retrieved from
593 http://www.sciencedirect.com/science/article/pii/S0008884610002632
594 Mehta, P. K. (1999). Concrete Technology for Sustainable Development. *Concrete*
595 *International, 21*, pp. 47-53.
596 Mlinárik, L., & Kopecskó, K. (2013). Impact of metakaolin-a new supplementary material—
597 on the hydration mechanism of cements. *Acta Tech Napocen Civil Eng Archit, 56*(2),
598 pp. 100-110.
599 Ng, S., & Justnes, H. (2015a). Influence of dispersing agents on the rheology and early heat of
600 hydration of blended cements with high loading of calcined marl. *Cement and Concrete*
601 *Composites, 60*, pp. 123-134.
602 Ng, S., & Justnes, H. (2015b). *Study on the Rheology of Fly Ash Versus Calcined Marl Blended*
603 *Cements with Polycarboxylate-Based Superplasticizers* 11th International Conference

on Super-plasticizers and Other Chemical Admixtures in Concrete, Ottawa, ON, Canada.
Nied, D., Stabler, C., & Zajac, M. (2015). *Assessing the Synergistic Effect of Limestone and Metakaolin.* Dordrecht.
Nielsen, O. B. (1994). Lithostratigraphy and sedimentary petrography of the Paleocene and Eocene sediments from the Harre borehole, Denmark. *Aarhus Geoscience, 1*, pp. 15-34.
Nielsen, O. B., Cremer, M., Stein, R., Thiébault, F., & Zimmermann, H. (1989). 8. ANALYSIS OF SEDIMENTARY FACIES, CLAY MINERALOGY, AND GEOCHEMISTRY OF THE PALEOGENE SEDIMENTS OF SITE 647, LABRADOR SEA. *Proceedings of the Ocean Drilling Program, Scientific Results, 105*, pp. 101-110.
Okoronkwo, M. U., & Glasser, F. P. (2016). Stability of strätlingite in the CASH system. [journal article]. *Materials and Structures, 49*(10), pp. 4305-4318. doi:10.1617/s11527-015-0789-x Retrieved from https://doi.org/10.1617/s11527-015-0789-x
Pöllmann, H., Da Costa, M. L., & Angelica, R. (2015). *Sustainable Secondary Resources from Brazilian Kaolin Deposits for the Production of Calcined Clays.* Dordrecht.
Rahhal, V., & Talero, R. (2008). Calorimetry of Portland cement with metakaolins, quartz and gypsum additions. *Journal of Thermal Analysis and Calorimetry, 91*(3), p 825.
Rakhimov, R. Z., Rakhimova, N. R., Gaifullin, A. R., & Morozov, V. P. (2017). Properties of Portland cement pastes enriched with addition of calcined marl. *Journal of Building Engineering, 11*, pp. 30-36. doi:https://doi.org/10.1016/j.jobe.2017.03.007 Retrieved from http://www.sciencedirect.com/science/article/pii/S2352710216303394
Ramachandran, V. S. (1988). Thermal analyses of cement components hydrated in the presence of calcium carbonate. *Thermochimica acta, 127*, pp. 385-394. doi:https://doi.org/10.1016/0040-6031(88)87515-4 Retrieved from http://www.sciencedirect.com/science/article/pii/0040603188875154
Rossen, J. E., Lothenbach, B., & Scrivener, K. L. (2015). Composition of C–S–H in pastes with increasing levels of silica fume addition. *Cement and Concrete Research, 75*, pp. 14-22. doi:https://doi.org/10.1016/j.cemconres.2015.04.016 Retrieved from http://www.sciencedirect.com/science/article/pii/S0008884615001222
Runkel, M., & Sturm, P. (2009). Pyrite roasting, an alternative to sulphur burning. *The Journal of the Southern African Institute of MIning and Metallurgy, 109*, pp. 491-497.
Sabir, B. B., Wild, S., & Bai, J. (2001). Metakaolin and calcined clays as pozzolans for concrete: a review. *Cement and Concrete Composites, 23*(6), pp. 441-454. doi:https://doi.org/10.1016/S0958-9465(00)00092-5 Retrieved from http://www.sciencedirect.com/science/article/pii/S0958946500000925
Schneider, M., Romer, M., Tschudin, M., & Bolio, H. (2011). Sustainable cement production—present and future. *Cement and Concrete Research, 41*(7), pp. 642-650. doi:https://doi.org/10.1016/j.cemconres.2011.03.019 Retrieved from http://www.sciencedirect.com/science/article/pii/S0008884611000950
Scrivener, K. (2015). *Calcined Clays for Sustainable Concrete, Proceedings of the 1st International Conference on Calcined Clays for Sustainable Concrete*: Springer.
Scrivener, K., Martirena, F., Bishnoi, S., & Maity, S. (2017). Calcined clay limestone cements (LC3). *Cement and Concrete Research*doi:https://doi.org/10.1016/j.cemconres.2017.08.017 Retrieved from http://www.sciencedirect.com/science/article/pii/S0008884617302454
Shayma'a, K. A., Malath, Q. A.-Q., Dalya Kh, A.-D., Firas, F. A.-H., & Abdul Wahab, A. A.-A. (2012). EVALUATION OF Al-AMIJ AND AL-HUSSAINIYAT CLAYSTONES (IRAQI WESTERN DESERT) FOR THE PRODUCTION OF POZZOLANA. *Iraqi*

Bulletin of Geology and Mining □□□□□□□□ □□□□□□□□□□ □□□□)1(*8,* □□□□□□□□, pp. 1-15.
Siddique, R., & Klaus, J. (2009). Influence of metakaolin on the properties of mortar and concrete: A review. *Applied Clay Science, 43*(3), pp. 392-400. doi:http://dx.doi.org/10.1016/j.clay.2008.11.007 Retrieved from http://www.sciencedirect.com/science/article/pii/S0169131708002706
. Standard CEN - EN 196-1 Methods of testing cement Part1: Determination of strength. (2005): European Committee for Standardization.
Talero, R., & Rahhal, V. (2009). Calorimetric comparison of portland cements containing silica fume and metakaolin: Is silica fume, like metakaolin, characterized by pozzolanic activity that is more specific than generic? *Journal of Thermal Analysis and Calorimetry, 96*(2), pp. 383-393.
Taylor, H. F. (1997). *Cement chemistry*: Thomas Telford.
Tironi, A., Castellano, C. C., Bonavetti, V. L., Trezza, M. A., Scian, A. N., & Irassar, E. F. (2014). Kaolinitic calcined clays – Portland cement system: Hydration and properties. *Construction and building materials, 64*, pp. 215-221. doi:https://doi.org/10.1016/j.conbuildmat.2014.04.065 Retrieved from http://www.sciencedirect.com/science/article/pii/S0950061814003821
Tironi, A., Scian, A. N., & Irassar, E. F. (2015). *Ternary Blended Cement with Limestone Filler and Kaolinitic Calcined Clay*. Dordrecht.
Tironi, A., Trezza, M. A., Scian, A. N., & Irassar, E. F. (2012). Kaolinitic calcined clays: Factors affecting its performance as pozzolans. *Construction and Building Materials, 28*(1), pp. 276-281.
Østnor, T., Justnes, H., & Danner, T. (2015). Reactivity and Microstructure of Calcined Marl as Supplementary Cementitious Material *Calcined Clays for Sustainable Concrete* (pp. 237-244): Springer.

Table 1: Mineralogical composition of the raw clays (Clay A and Clay B)

Phase (%)	A	B
Kaolinite	47	8
Smectite	—	54
Illite		4
Muscovite	2	
Chlorite	—	—
Quartz	18	4
Orthoclase	34	—
Calcite	—	25
Siderite	—	3
Pyrite	—	1

Table 2: Chemical composition and BET specific surface area of Clay A and B calcined at 800°C and the cement used in pastes.

Oxide (%)	A	B	Cement
SiO_2	60.6	48.7	19.9
Al_2O_3	30.0	17.8	4.8
Fe_2O_3	3.4	10.4	3.3
CaO	0.1	13.8	61.9
K_2O	3.2	2.4	1.0
Na_2O	—	0.7	0.5
MgO	0.4	2.8	2.7
MnO	0.0	0.2	
P_2O_5	0.1	0.2	0.2
TiO_2	0.4	1.0	
SO_3			3.3
Total	98.2	98.0	97.6
LOI	1.8	2.0	2.4
BET (m^2/g)	19	15	2

Table 3: Times of maximum thermal power (tmax) from the hydration of cement pastes with 20, 35 and 50 wt% calcined Clay A and B

PC + Clay A		PC + Clay B	
	t_{max} (h)		**t_{max} (h)**
PC	15.3	**PC**	15.3
20% A	12.5	**20% B**	16.5
35% A	9.3	**35% B**	15.1
50% A	7.3	**50% B**	13.8

692 Table 4: Amount of CH (measured from TG curves) in the pastes after 28 days of hydration

PC + Clay A		PC + Clay B	
	CH_{28d} (%)		**CH_{28d} (%)**
PC	16	**PC**	16
20% Clay A	10	**20% Clay B**	12
35% Clay A	5	**35% Clay B**	8
50% Clay A	2	**50% Clay B**	5

693

694 Table 5: WDX composition in atomic percent of points 1-8 indicated in Figure 11 and 12.

WDX_No.	Ca	Al	Si	Fe	K	O
1	12.9	9.4	5.3	0.8	0.3	70.8
2	16.5	8.9	1.1	0.5	0.1	72.1
3	11.3	9.4	5.9	0.6	0.2	72.5
4	11.5	10.1	6.7	0.5	0.2	70.9
5	11.7	10.6	5.5	0.5	0.1	71.4
6	16.9	9.1	0.8	1.5	0.1	71.1
7	16.7	6.9	2.8	0.5	0.3	72.2
8	16.1	5.8	0.9	1.6	0.0	75.2

695

696

697 Table 6: Relative strength of mortars containing calcined Clay A

	Relative compressive strength (%)			
Time	**REF**	**20%**	**35%**	**50%**
1 day	100	82	56	34
3 day	100	99	80	55
7 days	100	126	109	71
28 days	100	122	115	109

698

699

700 Table 7: Relative strength of mortars containing calcined Clay B

	Relative compressive strength (%)			
Time	**REF**	**20%**	**35%**	**50%**
1 day	100	81	64	43
3 day	100	88	77	58
7 days	100	95	92	84
28 days	100	107	106	95

701

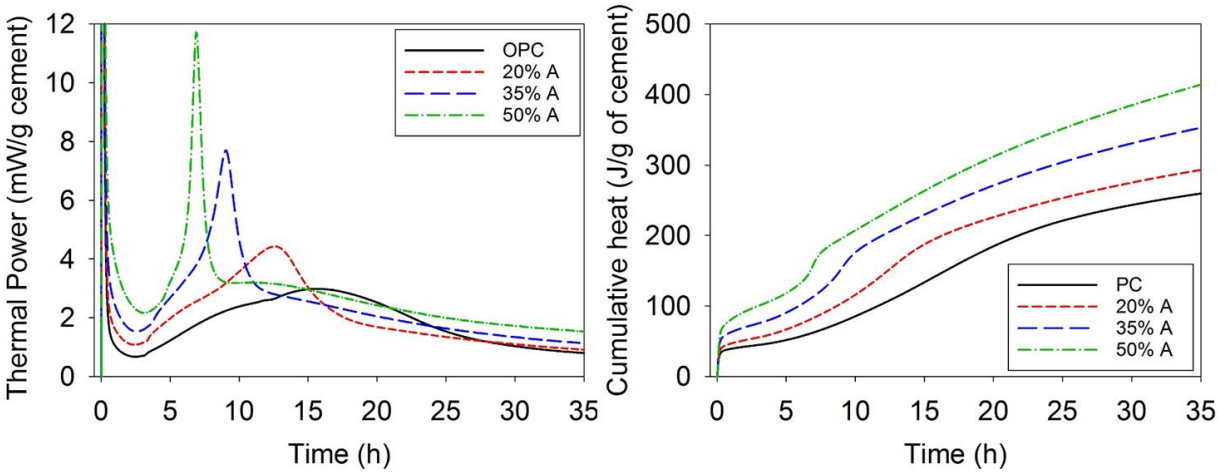

Figure 1: Thermal Power (left) and cumulative heat (right) of pastes of PC and 20, 35, 50 wt% calcined Clay A

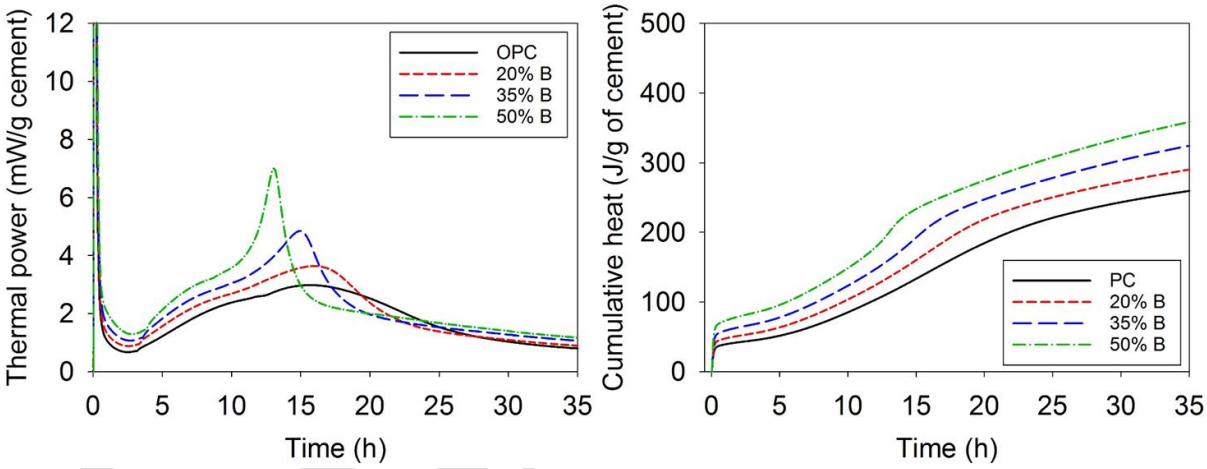

Figure 2: Thermal Power (left) and cumulative heat (right) of pastes of PC and 20, 35, 50 wt% calcined Clay B

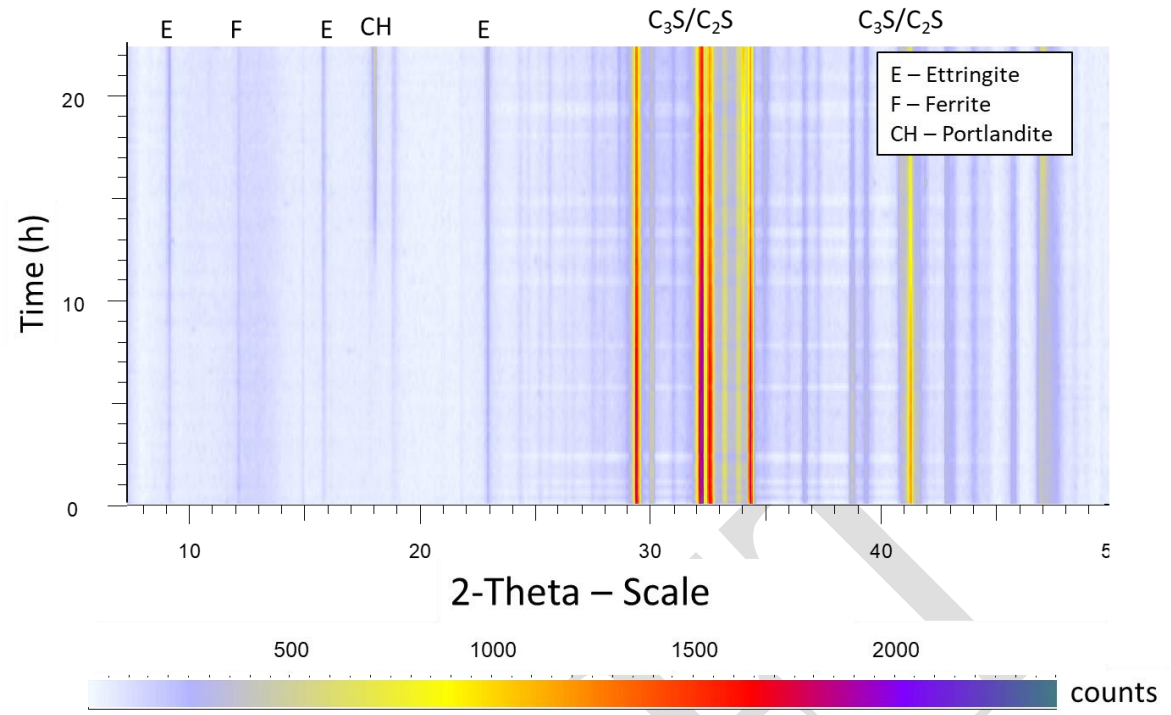

711

712 Figure 3: in-situ XRD level plot of hydrating PC paste during the first 24 h of hydration.
713 (E=ettringite; F=ferrite phase C_4AF; CH=portlandite)

714

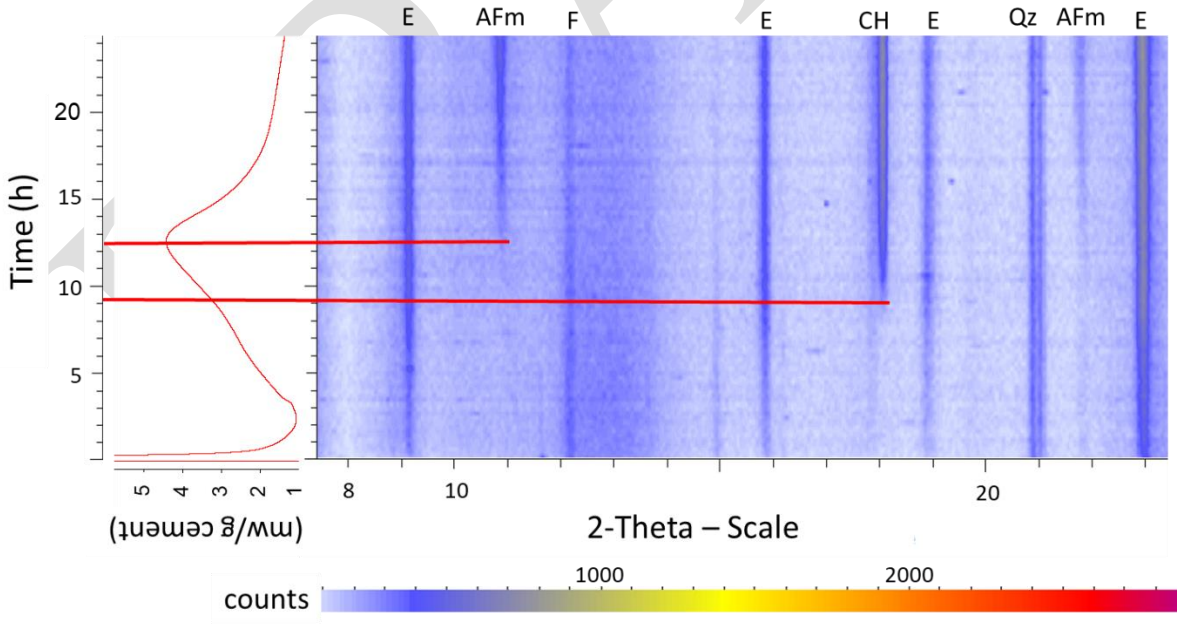

715

716 Figure 4: in-situ XRD level plot and thermal power curve of cement paste with 20 wt% calcined
717 Clay A hydrated for 24 h. (E=ettringite; AFm=hemi-carboaluminate; F=Ferrite phase C_4AF;
718 CH=portlandite; Qz=Quartz)

719

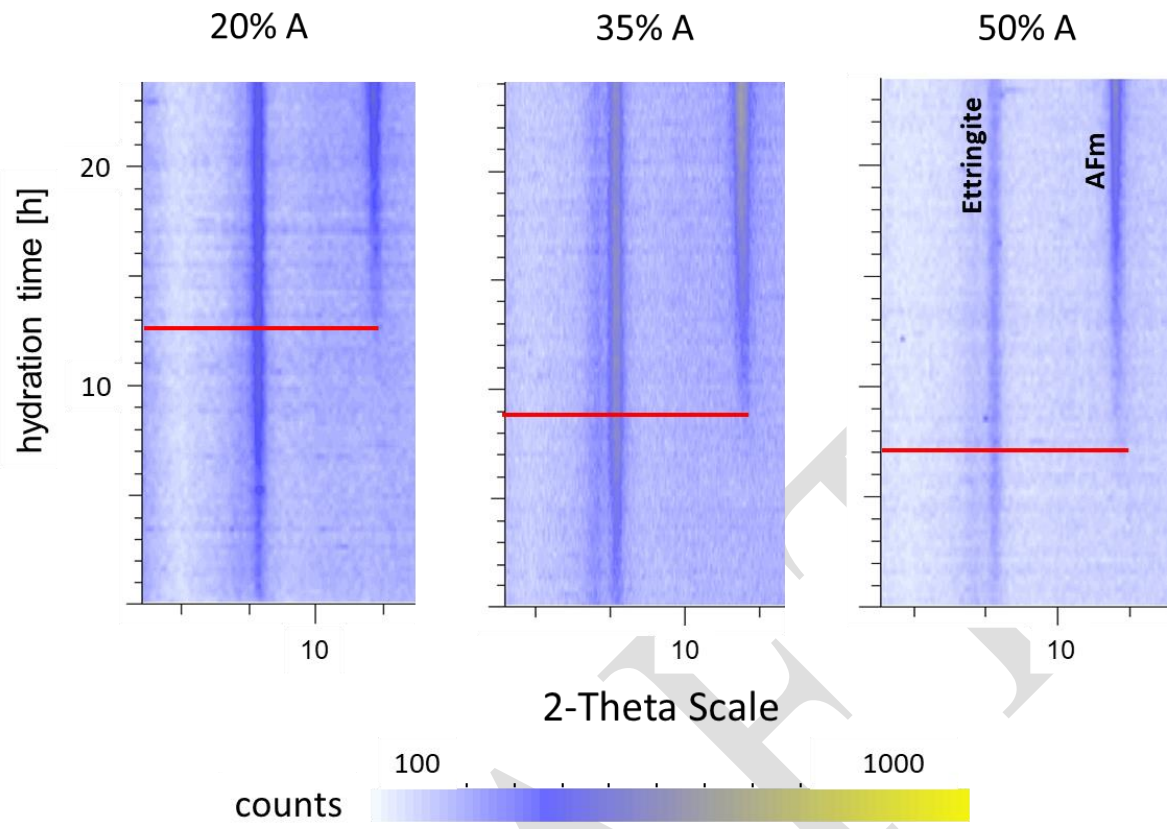

720

721 Figure 5: in-situ XRD levelplot of PC pastes with 20, 35 and 50 wt% Calcined Clay A hydrated

722 for 24 h at 20 °C. AFm = hemi-carboaluminate

723

724

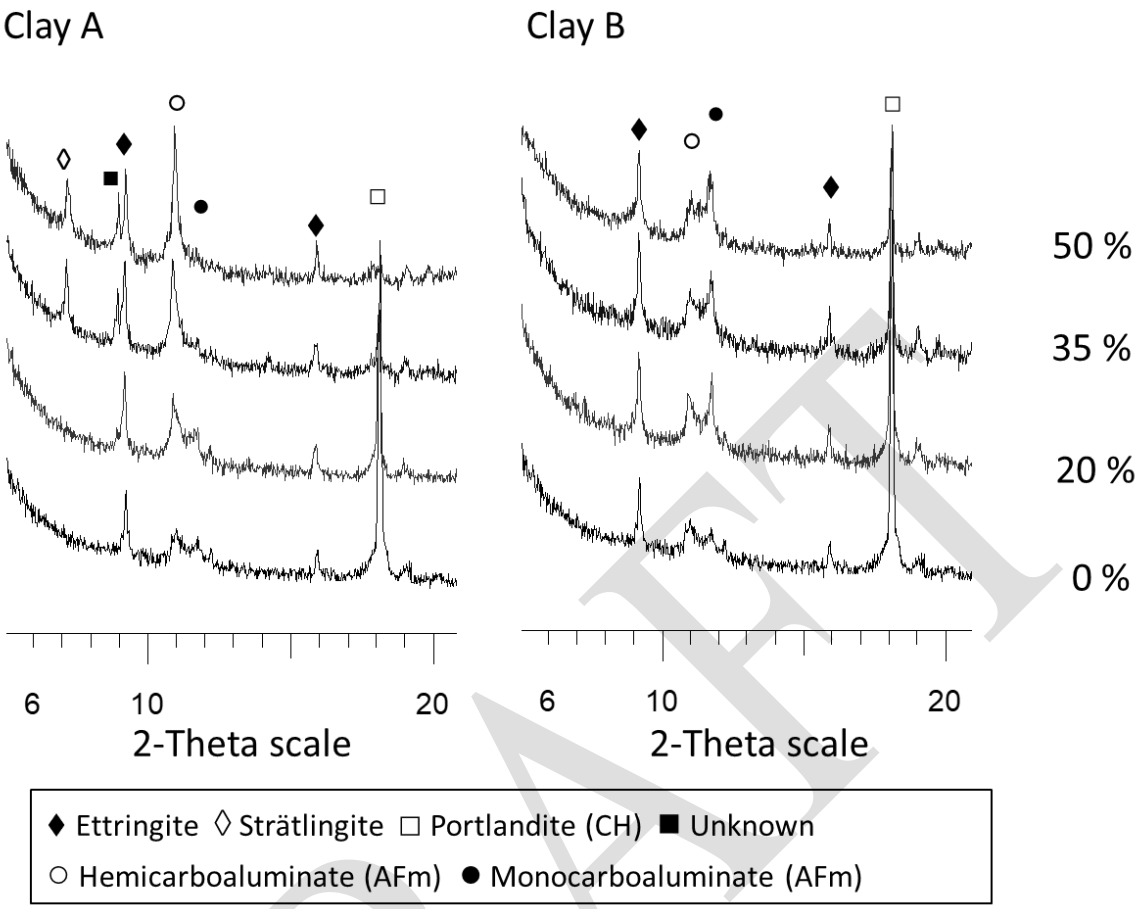

Figure 6: XRD diffractograms of cement pastes with 20, 35 and 50 wt% calcined Clay A (left) and calcined Clay B (right) hydrated for 28 days at 20 °C.

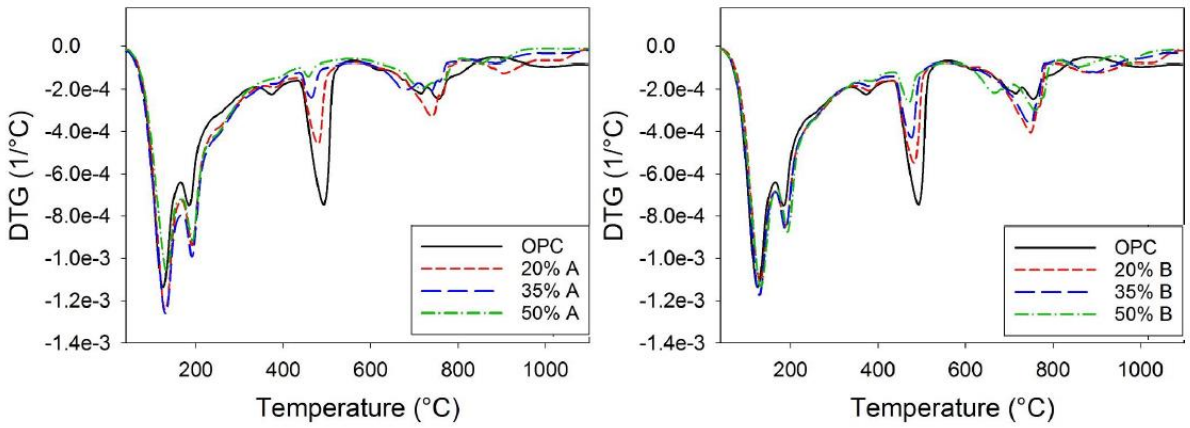

729

730 Figure 7: DTG of cement pastes with 20, 35 and 50 wt% calcined Clay A (left) and calcined
731 Clay B (right) hydrated for 28 days at 20°C.

732

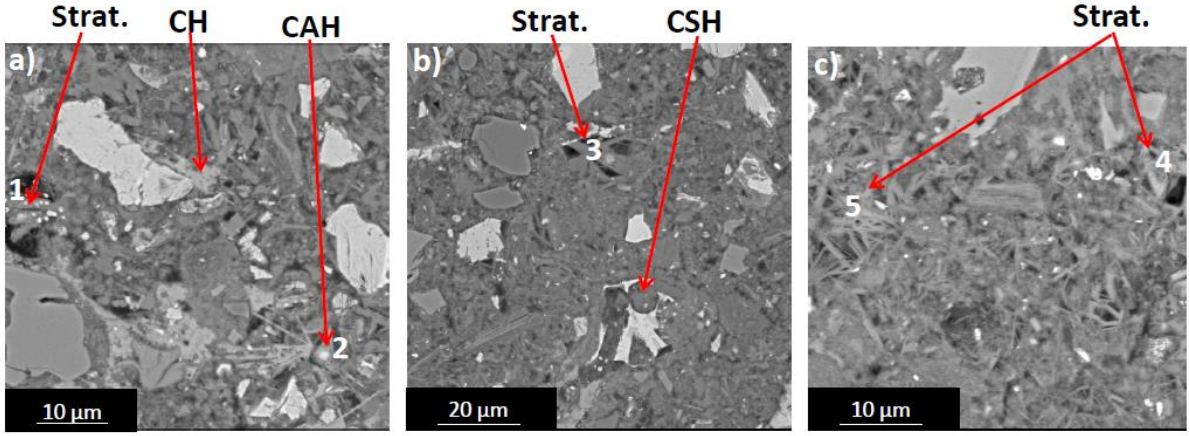

733

734 Figure 8: BSE images of cement pastes with a) 20, b) 35 and c) 50 wt% calcined Clay A
735 hydrated for 28 days at 20°C.

736

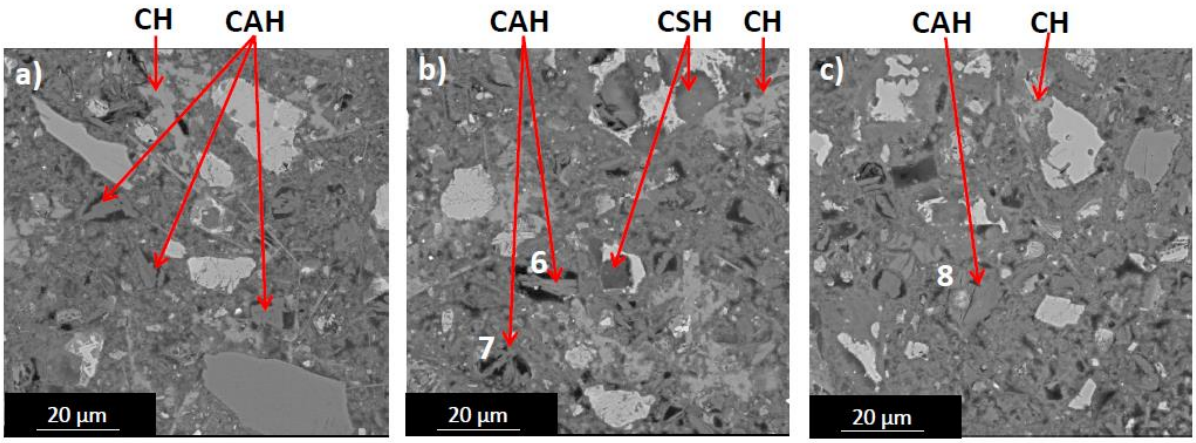

737

738 Figure 9: BSE images of cement pastes with a) 20, b) 35 and c) 50 wt% calcined Clay B
739 hydrated for 28 days at 20°C

740

741

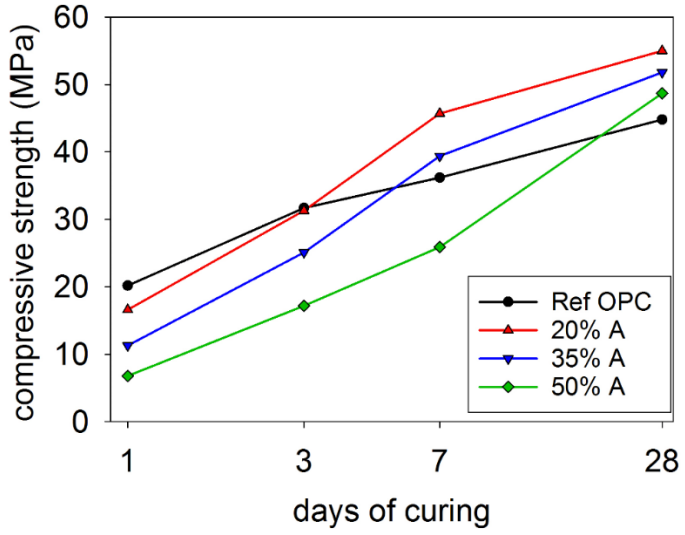

742

743 Figure 10: Compressive strength of standard mortars with 20, 35, 50 wt% replacement of PC
744 by calcined Clay A

745

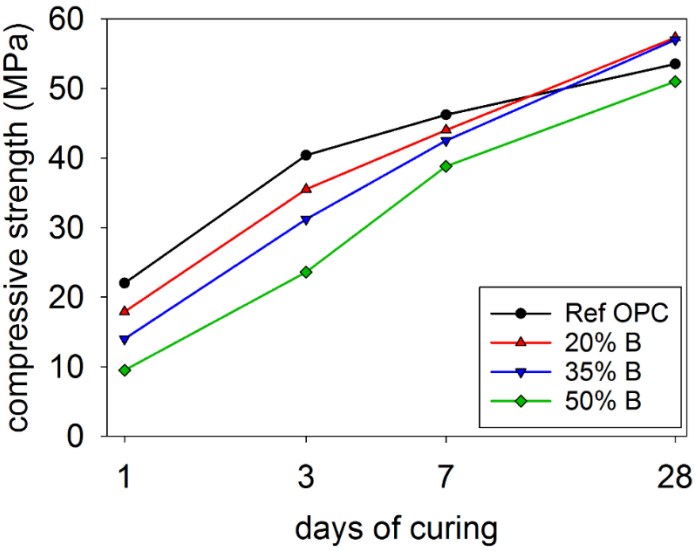

746

747 Figure 11: Compressive strength of standard mortars with 20, 35, 50 wt% replacement of PC
748 by Calcined Clay B

749